Modeling Kinetics of a Large-Scale Fed-Batch CHO Cell Culture by Markov Chain Monte Carlo Method

Zizhuo Xing
Biotechnology Process Development, Bristol-Myers Squibb Company, Syracuse, NY 13057

Nikki Bishop
Dept. of Chemical & Biological Engineering, Rensselaer Polytechnic Institute, Troy, NY 12180

Kirk Leister and Zheng Jian Li
Biotechnology Process Development, Bristol-Myers Squibb Company, Syracuse, NY 13057

DOI 10.1002/btpr.284
Published online October 15, 2009 in Wiley InterScience (www.interscience.wiley.com).

Markov chain Monte Carlo (MCMC) method was applied to model kinetics of a fed-batch Chinese hamster ovary cell culture process in 5,000-L bioreactors. The kinetic model consists of six differential equations, which describe dynamics of viable cell density and concentrations of glucose, glutamine, ammonia, lactate, and the antibody fusion protein B1 (B1). The kinetic model has 18 parameters, six of which were calculated from the cell culture data, whereas the other 12 were estimated from a training data set that comprised of seven cell culture runs using a MCMC method. The model was confirmed in two validation data sets that represented a perturbation of the cell culture condition. The agreement between the predicted and measured values of both validation data sets may indicate high reliability of the model estimates. The kinetic model uniquely incorporated the ammonia removal and the exponential function of B1 protein concentration. The model indicated that ammonia and lactate play critical roles in cell growth and that low concentrations of glucose (0.17 mM) and glutamine (0.09 mM) in the cell culture medium may help reduce ammonia and lactate production. The model demonstrated that 83% of the glucose consumed was used for cell maintenance during the late phase of the cell cultures, whereas the maintenance coefficient for glutamine was negligible. Finally, the kinetic model suggests that it is critical for B1 production to sustain a high number of viable cells. The MCMC methodology may be a useful tool for modeling kinetics of a fed-batch mammalian cell culture process. © 2009 American Institute of Chemical Engineers *Biotechnol. Prog.*, 26: 208–219, 2010
Keywords: kinetic model, MCMC sampling, bayesian parameter estimation, monod equation, Chinese hamster ovary cell culture

Introduction

A kinetic model that quantitatively elucidates the effects of limiting nutrients and repressing metabolites on cell growth and protein productivity can be used for simulation, optimization, and process control in cell cultures.[1–9] There are two limitations from models in the current literature. First, the kinetic models were developed from cell cultures at laboratory scale. Second, due to its nonlinear feature, a kinetic model has not been applied to a fed-batch cell culture system that includes multiple nutrients and metabolites with adequate accuracy. A modeling methodology that can be generally applicable to the fed-batch culture mode especially at manufacturing scale would be valuable for process control and productivity improvements.

A kinetic model can be structured or unstructured. A structured model attempts to explicitly describe intracellular processes in both a structural and physiological sense,[3,6] and thus offers the most realistic representation of a cell.[10] However, since the cell metabolism and responses to varying growth conditions are not thoroughly understood, a structured model is not applicable to most of cell lines. Therefore, the majority of the kinetic models in the literature are unstructured.[11] An unstructured model relies on concentrations of nutrients and metabolites in cultures, and neglects intracellular processes. The Monod-type relationship is a widely used unstructured model for cell growth and death rates. The Monod equation is based on the availability of limiting nutrients (such as glucose and glutamine) and inhibitors (such as lactate and ammonia) in a concentration-dependent pattern.[1,12] The maintenance coefficients of glucose and glutamine were introduced into the model, based upon the observation that the nutrient consumption rate was higher than the demand solely for cell growth in the stationary or cell death phase.[1,2]

Current address of Nikki Bishop: Department of Chemical and Biological Engineering, University of Colorado, Boulder, CO 80309.
Correspondence concerning this article should be addressed to Z. J. Li at zhengjian.li@bms.com.

Unstructured kinetic models have also been used to predict recombinant protein productivity in mammalian cell cultures.[1,13–15] Different studies have reported antibody production to be growth- and nongrowth-associated.[9] However, the highest specific antibody production rate was often observed at a low specific growth rate in many cases regardless of cell culture mode being used.[16–19] Furthermore, it has been reported that the specific antibody production rate was highest in the G1-phase[20] or G0-phase of the cell cycle.[21] The influence of substrate concentrations (glucose and glutamine) on recombinant protein productivity was found to be cell line dependent. It was reported that the correlation between nutrient concentrations and protein productivity could be positive,[19,22–23] not significant,[11,24] or negative[25] in mammalian cell cultures. Toxic metabolites, such as ammonia and lactate, have been reported to not significantly affect antibody productivity.[26–27]

To estimate kinetic parameters, a continuous culture has been used to achieve steady states, which simplifies the calculations.[11] In the continuous culture, multiple steady states at various growth rates and environmental conditions can be established.[10] For example, while a continuous hybridoma cell culture was shifted from one steady state at 8.3 mM glucose into another steady state at 12.2 mM glucose, the levels of glutamine, lactate, and ammonia were maintained constant. With the assumption that metabolites independently affect specific cell growth rate, the Monod constant K_{glc} can be calculated from the dilution rate and the residual glucose concentration in the multiple steady states.[5] However, continuous cultures with multiple steady states are not easy to operate even in laboratory bioreactors. Furthermore, as fed-batch cultures are widely used for manufacturing processes in the biotechnology industry, the model developed from continuous cultures may not truly reflect cell physiological states in fed-batch cell culture processes.

Although kinetic models have been reported for batch cell cultures,[2,22,28,29] it is rather difficult to estimate the large number of the Monod-type parameters from batch culture data by nonlinear least-square-error methodology.[10,30] The difficulties were either no single solution or insufficient accuracy.[31–33] To address the nonlinear features of kinetics in cell culture, neural networks were used to simulate the kinetic model.[8,9] Although neural networks were able to simulate time profiles of variables in cell culture, they were unable to estimate parameters in a physiological sense. Recently, the Markov chain Monte Carlo method (MCMC) was employed to estimate nonlinear process parameters in microbial fermentation and cell physiology studies. For example, physiological state variables were estimated for feeding strategy optimization in a fed-batch *Bacillus subtilis* fermentation.[34] More recently, MCMC was used for Bayesian parameter estimation in *Escherichia coli* fermentation[35] and to estimate parameters associated with glucose metabolism in humans.[36] With the advances in solving the nonlinear differential equations numerically, it may be feasible to estimate parameters of a kinetic model directly from a fed-batch mammalian cell culture process using the MCMC method.

This work reports the application of the MCMC method to develop a model that accurately described the kinetics of a large-scale fed-batch Chinese hamster ovary (CHO) cell culture process. This model consists of six differential algebraic equations (DAEs) describing culture dynamics for viable cell density and concentrations of glucose, glutamine, ammonia, lactate, and the antibody fusion protein B1 (B1). The structure of the kinetic model is similar to a neural network. Unlike a hidden layer of the ordinary neural network, DAEs explicitly describe the kinetics of cell cultures in a physiological sense. The kinetic model has 18 parameters, six of which were calculated from the cell culture data, whereas the other 12 were estimated from a training data set that comprises of seven cell culture runs in 5,000-L bioreactors using a MCMC method. The model was then applied to predict time profiles for the six variables in seven different cell culture runs in 5,000-L bioreactors (validation data set 1). Due to the GMP environment of 5,000-L facilities, a perturbation of cell culture condition was not allowed to be performed at this scale. Alternatively, we tested the model in 500-L bioreactors using the scaled down model. The results showed different profiles for the variable values (validation data set 2) due to the perturbation of the cell culture condition. Those two validation sets were used to examine general applicability of the model to the current CHO fed-batch cell culture process. The implications of the kinetic model to aid in medium design and process improvement are also discussed.

Materials and Methods

Cell line and bioreactor operation

The proprietary CHO cell line, basal and feeding media, and production scale process were previously described.[37,38] Cell culture runs were carried out in 5,000-L and 500-L bioreactors (Feldmeier Equipment, Syracuse, NY). The 500-L bioreactors were run under the scaled-down strategy with the same bioreactor configuration, the scaled agitation rate, and the same volume per volume per minute of air flow rate. Cell cultures were seeded at a viable cell density of $\sim 0.2 \times 10^6$ cells mL^{-1} and operated at a starting temperature of 37°C. The temperature, pH, and dissolved oxygen were controlled with an internally developed process. Cell cultures were performed in fed-batch mode with daily feeding from the first day though the end of cultivation period to maintain the proprietary glucose concentration.

Variables and analytical methods

Cell culture samples were taken daily before feeding. Thus, the measured values of six variables ($\mathbf{X2}^{(d)}$) shown in Eq. 1 are defined as the concentrations before feeding (prefeed values). Viable cell density (X_V) was determined by the average of eight cell counts. Cell counts were performed by trypan blue dye exclusion using a hemocytometer. Concentrations of glucose ([GLC]), glutamine ([GLN]), lactate ([LAC]), and ammonia ([AMM]) were measured using a NOVA Bioprofile 400 (NOVA Biomedical, Waltham, MA). B1 protein titers ([B1]) were measured by affinity chromatography using an internally developed method.

$$\mathbf{X2}^{(d)} = \left[[B1]_2^{(d)} \; [GLC]_2^{(d)} \; [GLN]_2^{(d)} \; [LAC]_2^{(d)} \; [AMM]_2^{(d)} \; X_{V,2}^{(d)} \right] \qquad d = 0, 1, \ldots 13 \qquad (1)$$

The postfeed values for the six variables ($\mathbf{X1}^{(d)}$) were defined by Eq. 2 and calculated by Eq. 3, which adjusts the value of $\mathbf{X2}^{(d)}$ based on the feed volume and the concentration in the feed for that variable. In this equation, $x1_i$ and $x2_i$ ($i = 1, 2, \ldots, 6$) are post and prefeed values of the ith variable, respectively. V, V_f, and CF_i are culture volume (L), feed volume (L), and the concentration of the ith variable in the feed medium (mM).

$$\mathbf{X1}^{(\mathrm{d})} = \left[[B1]_1^{(d)}\ [\mathrm{GLC}]_1^{(\mathrm{d})}\ [\mathrm{GLN}]_1^{(d)}\ [\mathrm{LAC}]_1^{(d)}\ [\mathrm{AMM}]_1^{(d)}\ X_{V,1}^{(d)}\right] \quad d = 0, 1, \ldots 13 \qquad (2)$$

$$x1_i^{(d)} = \frac{x2_i^{(d)} \cdot V^{(d)} + V_f^{(d)} \cdot \mathrm{CF}_i}{V^{(d)} + V_f^{(d)}} \qquad (3)$$

The yields, $Y_{X_V/\mathrm{glc}}$, $Y_{X_V/\mathrm{gln}}$, $Y_{\mathrm{lac/glc}}$, and $Y_{\mathrm{amm/gln}}$, were calculated in the first 6 days post inoculation ($d = 6$) by Eq. 4, which was adopted from literature reports.[39,40] In this equation, $x2_i$ is the ith element of the vector **X2** (Eq. 1). The value of $\sum_{d=0}^{5} V_f^{(d)} \cdot CF_j$ is the total amount of substrate $x2_j$ ($j = 2$, 3) being fed in the first 5 days post inoculation. The parameters $\mu_{\max}$ and k_d are determined from 112 historical cell culture runs in 5,000-L bioreactors. For each cell culture run, the values of μ_{app} were calculated as the slope of ln (X_V) vs. time plot (Eq. 5) for time periods of 0–96 h and 264–312 h. The maximum rate constants for cell growth ($\mu_{\max}$) and cell death (k_d), were defined as the upper limit for the absolute μ_{app} values calculated for 0–96 h and 264–312 h, respectively, using the 95% confidence level under the one-tail hypotheses.

$$Y_{x2_k/x2_j} = \left| \frac{x2_x^{(6)} \cdot V^{(6)} - x2_k^{(0)} \cdot V^{(0)}}{\left(x2_j^{(0)} \cdot V^{(0)} - x2_j^{(6)} \cdot V^{(6)}\right) + \sum_{d=0}^{5} V_f^{(d)} \cdot \mathrm{CF}_j} \right| \quad k = 4, 5, 6;\ j = 2, 3 \qquad (4)$$

$$\ln(X_V) = \mu_{\mathrm{app}} t \qquad (5)$$

Kinetic model

The kinetic model was expressed as six DAEs by Eq. 6, which were adopted from literature reports.[21,40] The mass balance for titer, [B1], was applied only after 144 h, as earlier samples are typically below the concentration range for the assay. In addition, since the highest specific antibody production rate was observed in the G1 or G0-phase of the cell cycle based on literature reports,[20,21] the fraction of arrested viable cells was introduced into the mass balance equation for [B1]. The fraction of viable cells ($X_V^{(d)}$) that are not undergoing propagation by the next sampling time ($t^{(d+1)}$) was estimated by the term ($1 - \mu/\mu_{\max}$).

$$\begin{cases} \dfrac{dX_V}{dt} = (\mu - \mu_d) \cdot X_V \\ \dfrac{d[\mathrm{GLC}]}{dt} = -\left((\mu - \mu_d)/Y_{X_V/\mathrm{glc}} + m_{\mathrm{glc}}\right) \cdot X_V \\ \dfrac{d[\mathrm{GLN}]}{dt} = -\left((\mu - \mu_d)/Y_{X_V/\mathrm{gln}} + m_{\mathrm{gln}}\right) \cdot X_V - d_{\mathrm{gln}}[\mathrm{GLN}] \\ \dfrac{d[\mathrm{LAC}]}{dt} = Y_{\mathrm{lac/glc}} \cdot \left((\mu - \mu_d)/Y_{X_V/\mathrm{glc}} + m_{\mathrm{glc}}\right) \cdot X_V \\ \dfrac{d[\mathrm{AMM}]}{dt} = Y_{\mathrm{amm/gln}} \cdot \left((\mu - \mu_d)/Y_{X_V/\mathrm{gln}}\right) \cdot X_V - r_{\mathrm{amm}} \cdot X_V + d_{\mathrm{gln}}[GLN] \\ \dfrac{d[\mathrm{B1}]}{dt} = Q_{B1} \cdot X_V \cdot \left(1 - \dfrac{\mu}{\mu_{\max}}\right) \cdot [B1] \end{cases} \qquad (6)$$

The values for μ and μ_d, were calculated by Eq. 7.[1,2,41] As previously reported,[38] inhibition to cell growth became significant when ammonia and/or lactate reached concentrations of 5.1 and 58 mM, respectively (threshold values). Therefore, the ammonia or lactate was considered in Eq. 7 only when the concentration exceeded 90% of their threshold value, or 4.6 and 52 mM for ammonia and lactate, respectively.

$$\begin{cases} \mu = \mu_{\max} \dfrac{[\mathrm{GLC}]}{K_{\mathrm{glc}} + [\mathrm{GLC}]} \cdot \dfrac{[\mathrm{GLN}]}{K_{\mathrm{gln}} + [\mathrm{GLN}]} \cdot \dfrac{\mathrm{KI}_{\mathrm{lac}}}{KI_{\mathrm{lac}} + [\mathrm{LAC}]} \cdot \dfrac{\mathrm{KI}_{\mathrm{amm}}}{KI_{\mathrm{amm}} + [\mathrm{AMM}]} \\ \mu_d = k_d \cdot \dfrac{[\mathrm{LAC}]}{\mathrm{KD}_{\mathrm{lac}} + [\mathrm{LAC}]} \cdot \dfrac{[\mathrm{AMM}]}{\mathrm{KD}_{\mathrm{amm}} + [\mathrm{AMM}]} \end{cases}$$

where

$$\begin{cases} \textit{if } [\mathrm{AMM}] \le 4.6 \text{ mM then } \mathrm{KI}_{\mathrm{amm}} \gg [\mathrm{AMM}], \\ \quad \mathrm{KD}_{\mathrm{amm}} \gg [\mathrm{AMM}] \\ \textit{if } [\mathrm{LAC}] \le 52 \text{ mM then } \mathrm{KI}_{\mathrm{lac}} \gg [\mathrm{LAC}],\ \mathrm{KI}_{\mathrm{lac}} \gg [\mathrm{LAC}] \end{cases} \qquad (7)$$

Other restrictions were applied to the μ, m_{glc}, and m_{gln} in the kinetic model. The cell death phase was defined after the viable cell density declined by 10% of the peak viable cell density in a cell culture run. It was assumed that $\mu = 0$ during the cell death phase. Since m_{glc} and m_{gln} are negligible during exponential growth,[1,2,11] it was assumed $m_{\mathrm{glc}} = 0$ and $m_{\mathrm{gln}} = 0$ when $d \le 6$. In addition, the value of m_{gln} is a function of glutamine (Eq. 8) in mammalian cell cultures as described in literature reports.[11,40]

$$m_{\mathrm{gln}} = \frac{a_1[\mathrm{GLN}]}{a_2 + [\mathrm{GLN}]} \qquad (8)$$

The DAEs were used for kinetic modeling of a batch hybridoma cell culture.[40] Since our cell cultures were performed in fed-batch mode with a daily bolus feed addition, the time period between two successive feedings ($t^{(d)}$, $t^{(d+1)}$) was considered as a batch culture and Eq. 6 was applied to each time period as shown in Figure 1B. Although the model structure is similar to a neural network as described in the literature,[8] the DAEs replaced the hidden layer of an ordinary neural network. Unlike a hidden layer of the ordinary neural network, the DAEs explicitly describe the cell culture kinetics in a physiological sense. The inputs for the calculations consists of initial estimates for each parameter (proposal parameters (θ)), known constants (**P**), and the postfeeding values of the six variables at $t^{(d)}$ ($\mathbf{X1}^{(d)}$). The outputs are the prefeed values for the six variables at $t^{(d+1)}$ ($\mathbf{X2}^{(d+1)}$). The ODE23 function of MATLAB Version 7.5 (Mathwork, Natick, MA) was used to numerically solve Eq. 6 for each time period.

$$\boldsymbol{\theta} = [K_{\mathrm{glc}}\ K_{\mathrm{gln}}\ KI_{\mathrm{amm}}\ KI_{\mathrm{lac}}\ KD_{\mathrm{amm}}\ KD_{\mathrm{lac}}\ m_{\mathrm{glc}}\ Q_{B1}\ d_{\mathrm{gln}}\ R_{\mathrm{amm}}\ a_1\ a_2] \qquad (9)$$

$$\mathbf{P} = [\mu_{\max}\ k_d\ Y_{X_V/\mathrm{glc}}\ Y_{X_V/\mathrm{gln}}\ Y_{\mathrm{lac/glc}}\ Y_{\mathrm{amm/gln}}] \qquad (10)$$

Markov chain Monte Carlo method

The parameter estimation was performed for each cell culture run using the MCMC sampling procedure as presented

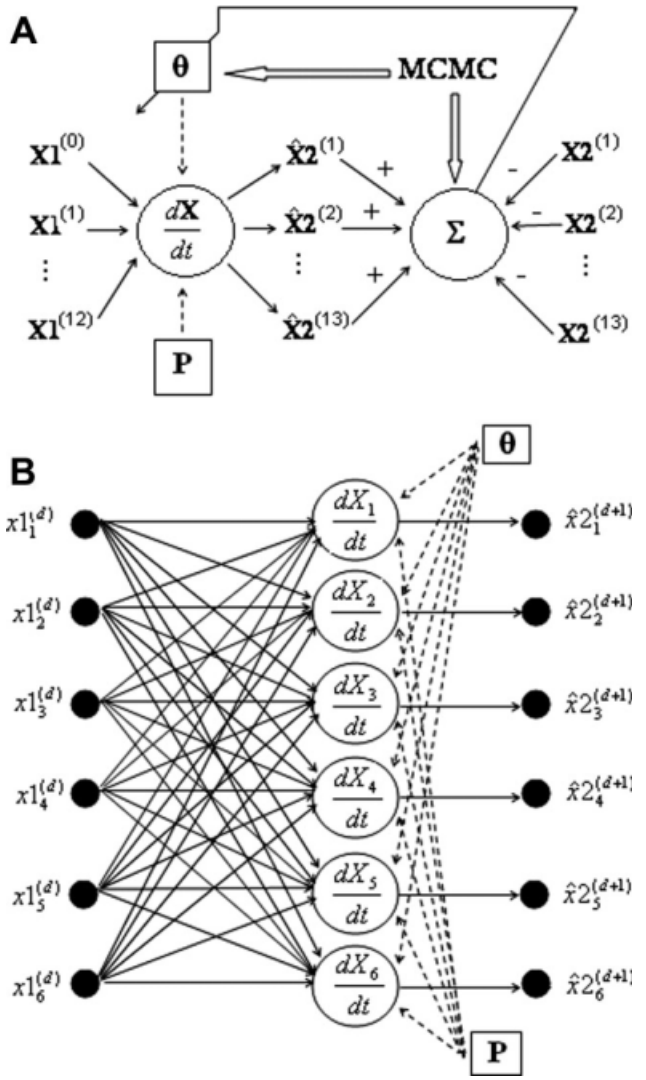

Figure 1. Schematic representation for parameter estimation using MCMC methodology.

(A) MCMC sampling procedure creates a set of proposal parameters (θ) and provides the acceptance function to evaluate θ using a feed-back approach. (B) For each period ($t_{(d)}$, $t_{(d+1)}$), the simulated values at $t_{(d+1)}$ were calculated by Eq. 6.

in Table 1. To facilitate the reliability test described in the next section, three MCMC sampling trains were used for each cell culture run. Each train was initiated from a different set of parameters $\theta^{(0)}$ that will be described in detail in the results section.

For each MCMC sampling train, 10,000 iterations were performed. The Monte Carlo sampling method was used to generate a set of proposal parameters for an iteration of MCMC sampling procedure. Using the proposal parameters, the simulated values of the six variables at 13 sampling times can be calculated by Eq. 6 as shown in Figure 1. The proposal parameters and simulated values of the six variables were then used to calculate the acceptance function and to determine adequacy of the proposal parameters using Eq. 11. The accepted parameters were then assigned as the initial parameters for the next iteration. After completing 10,000 iterations, the outcomes of the first 5,000 iterations were discarded to minimize the influence of the initial proposal parameters $\theta^{(0)}$.[42] The average value of a model parameter

Table 1. Basic Procedure for Model Parameter Estimation by the MCMC Methodology[42]

1. Function MCMC_Main_Program
   1.1 For train $k = 1, 2, 3$ do
      1.1.1. Initialize the parameter $\theta^{(0)}$ and assign $\theta^{initial} = \theta^{(0)}$
      1.1.2. Estimate the variable values ($X^{initial}$) using $\theta^{initial}$ by Eq. 6 shown in Figure 1B
      1.1.3. For iteration $j = 1, 2, \ldots, 10{,}000$ do
         1.1.3.1. For parameter_number $i = 1, 2, \ldots, 10$ do
            1.1.3.1.1. Draw a proposal $\theta_i^{(k)}$ from $U(\theta_i^{min}, \theta_i^{max})$ and assign
            $$\boldsymbol{\theta}^{proposal} = \left[\theta_j^{(k)} \; for \; j \prec i, \; \theta_i^{(k)}, \; \theta_j^{(k-1)} \; for \; j \succ i\right]$$
            1.1.3.1.2. Call evaluate_proposal_parameters
         1.1.3.2. Record $\theta^{(j)} = \theta^{transfer}$
   1.2. For parameter_number $i = 1, 2, \ldots, 10$ do
   $$\theta_i = \frac{1}{5{,}000} \sum_{j=5{,}001}^{10{,}000} \theta_i^{(j)}$$
2. Function Evaluating_Proposal_Parameters
   2.1. Calculate the variable values ($X^{proposal}$) using $\theta^{proposal}$ by Eq. 6 shown in Figure 1B
   2.2. Compute the acceptance probability (A) by Eq. 11
   2.3. Determine acceptance of $\theta^{transfer}$ and $X^{transfer}$
   2.4. Assign $\theta^{initial} = \theta^{transfer}$ and $X^{initial} = X^{transfer}$

from the remaining 5,000 iterations was then defined as the estimated parameter from this cell culture run.

$$A(\boldsymbol{\theta}^{proposal}, \boldsymbol{\theta}^{initial}) = \min\left(1, \frac{f(X2 \mid \boldsymbol{\theta}^{proposal}) \; \Pr(\boldsymbol{\theta}^{initial} \mid \boldsymbol{\theta}^{proposal}, \sigma_{\boldsymbol{\theta}^{proposal}})}{f(X2 \mid \boldsymbol{\theta}^{initial}) \; \Pr(\boldsymbol{\theta}^{proposal} \mid \boldsymbol{\theta}^{initial}, \sigma_{\boldsymbol{\theta}^{initial}})}\right)$$

$$\text{if } U(0,1) \geq A(\theta^{proposal}, \theta^{initial}), \text{ set } \theta^{accepted} = \theta^{proposal}$$

$$\text{Otherwise, set } \theta^{accepted} = \theta^{initial} \tag{11}$$

where

$$\begin{cases} f(X2 \mid \boldsymbol{\theta}) = \prod_{i=1}^{6} \prod_{d=4}^{14} \frac{1}{\sigma_i^{(d)}\sqrt{2\pi}} \exp\left(-\frac{1}{2}\left(\frac{\hat{x}2_i^{(d)} - x2_i^{(d)}}{\sigma_i^{(d)}}\right)^2\right) \\ \log(\boldsymbol{\theta}) \sim N(\log(\hat{\boldsymbol{\theta}}), \sigma_{\hat{\boldsymbol{\theta}}}) \\ \sigma_{\hat{\boldsymbol{\theta}}} = \log(\hat{\boldsymbol{\theta}}) \cdot \tau \\ \tau \sim U(0,1) \end{cases} \tag{12}$$

As shown in Eq. 11, the acceptance criterion was based on the current proposal parameter values (the *n*th iteration) and the accepted parameter values from the previous iteration [e.g., the $(n-1)$th iteration], whereas neglecting the prior iterations, making the outcomes of the MCMC sampling as a Markov chain. In Eq. 11, the candidate distribution density $f(\mathbf{X}|\boldsymbol{\theta})$ can be calculated by Eq. 12, of which $\hat{x}_i^{(d)}$ and $x_i^{(d)}$ were the simulated and measured values, respectively, for the *i*th variable as measured on the *d*th day of a cell culture run. The value of $\sigma_i^{(d)}$ was the standard deviation for the corresponding measurement from the 14 cell culture runs in 5,000-L bioreactors used in this study. The proposal distribution $\Pr(\boldsymbol{\theta} \mid (\hat{\boldsymbol{\theta}}, \sigma_{\boldsymbol{\theta}})$ was a log-normal distribution.[43] The standard deviation σ_θ was calculated from $\log(\hat{\boldsymbol{\theta}})$ and coefficient of variation (τ). The τ values were sampled from the uniform distribution U(0, 1).

Reliability assessments of the kinetic model

To evaluate the reliability of the MCMC method, the convergence assessment was performed to ensure the sequence

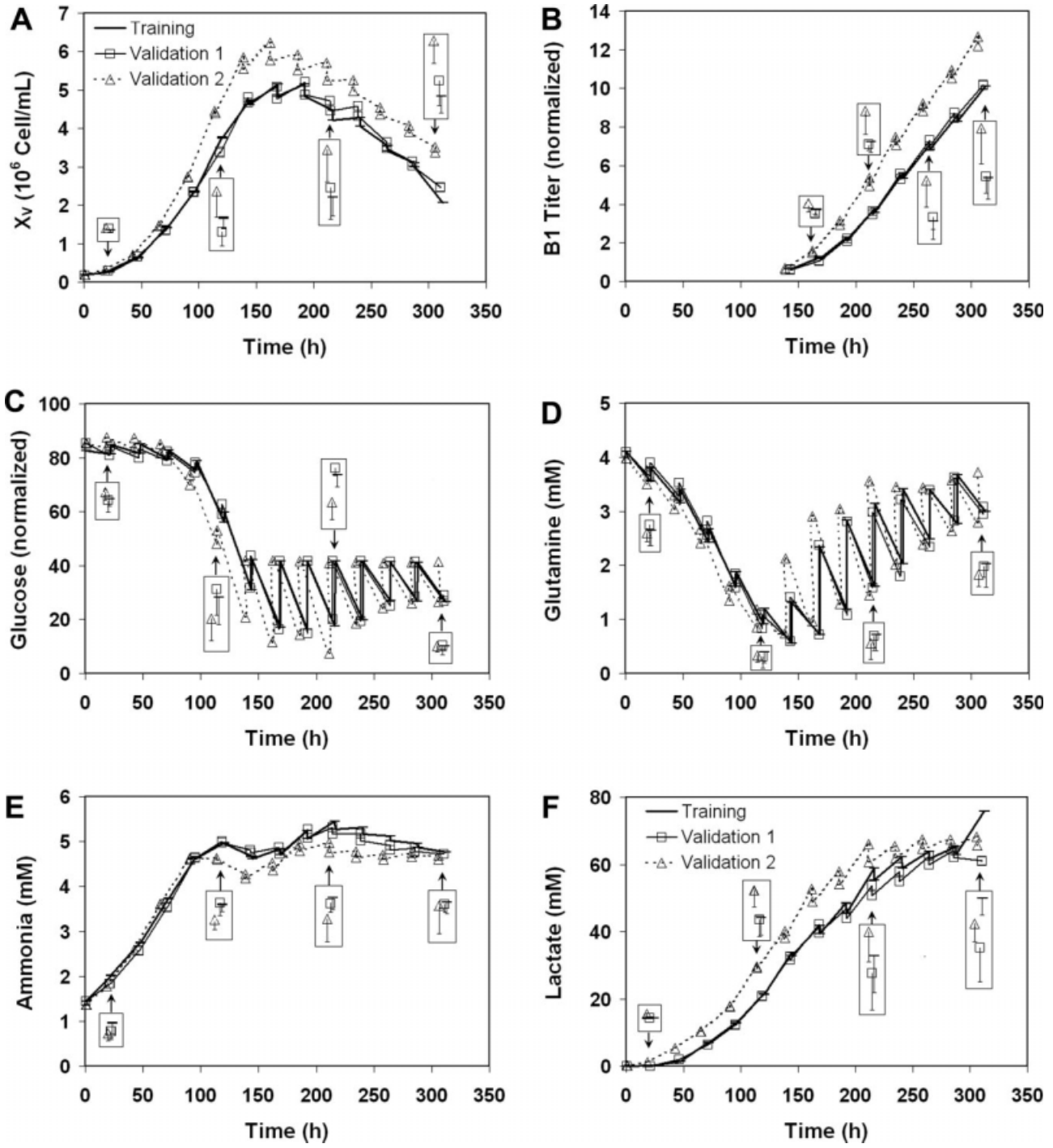

Figure 2. Time profiles of the six variables in CHO cell cultures.

The cell cultures of the training data set (Training) and the first validation data set (Validation 1) were performed in 5,000-L bioreactors, whereas those of the second validation data set (Validation 2) were performed in 500-L bioreactors. Each data set comprised seven cell culture runs. The bar of each symbol in a box is the standard deviation of prefeeding samples of seven cell culture runs at the pointed time. Four sampling times were presented as example for each variable.

of estimated parameters approached a steady state (converged). As mentioned in the last section, MCMC was performed on three independent sampling trains with different initial proposal parameters $\theta^{(0)}$. The potential scale reduction factor ($PSRF_i$) for a model parameter (θ_i) was calculated for convergence assessment by Eq. 13. If the PSRF values of all 12 parameters approached one, the MCMC sampling achieved a steady state, suggesting that the estimated 12 model parameters were equivalent among three independent sampling trains.[44,45] The variables required for PSRF calculation were defined by Eq. 14. The value of the *i*th parameter estimated from the *j*th iteration of the *k*th sampling train is represented by $\theta_i^{(kj)}$, and $\overline{\theta}_i^{(k.)}$ and $\overline{\theta}_i$ represents the average values of the *i*th parameter from the *k*th train and total three trains, respectively.

$$\mathrm{PSRF}_i = \frac{\hat{V}_i}{W_i} \tag{13}$$

Table 2. Measured Constants Used in the Kinetic Model (Eq. 6)

Constants	Values
μ_{max} (h^{-1})	0.029
k_d (h^{-1})	0.016
$Y_{Xv/glc}$ (10^{11} cells mol^{-1})	1.69 ± 0.37
$Y_{Xv/gln}$ (10^{11} cells mol^{-1})	9.74 ± 1.65
$Y_{lac/glc}$ (mol mol^{-1})	1.23 ± 0.06
$Y_{amm/gln}$ (mol mol^{-1})	0.67 ± 0.06

where

$$\begin{cases} \hat{V}_i = \dfrac{n-1}{n} W_i + \dfrac{B_i}{n} + \dfrac{B_i}{mn} \\ \dfrac{B_i}{n} = \displaystyle\sum_{k=1}^{m} (\bar{\theta}_i^{(k)} - \bar{\theta}_i)^2 / (m-1) \\ W_i = \dfrac{1}{m(n-1)} \displaystyle\sum_{k=1}^{m} \sum_{j=n+1}^{2n} (\theta_i^{(kj)} - \bar{\theta}_i^{(k.)})^2 \end{cases} \quad (14)$$

Two assessments were made for the accuracy and applicability of the kinetic model. As shown in Eqs. 11 and 12, the accuracy of parameter estimation by the MCMC method was based on the fit of the simulated and measured values of the six variables in the training data-set. A simple regression analysis was used to assess the accuracy for each variable,[46] of which 91 pairs of the simulated and measured values (7 cell culture runs × 13 days) were compared. To evaluate the applicability, the developed model was then applied to seven different cell culture runs in 5,000 L-bioreactors to predict the time profiles of the six variables (Validation 1). To further evaluate if the model was applicable to a perturbation of the cell culture condition, the developed model was applied to seven cell culture runs in 500-L bioreactors to predict the time profiles of the six variables (Validation 2). Data from the 500 L pilot scale bioreactors were necessary because such perturbations were not allowed in the GMP environment of the 5,000-L bioreactors. As mentioned above, the 500-L bioreactors were run under the scaled-down strategy with the same bioreactor configuration, the scaled agitation rate, and the same volume per volume per minute of air flow rate. The fit of predicted profiles to the measured profiles would suggest that the kinetic model to be generally applicable to the current CHO cell culture process.

Results and Discussion

Variables, constants, and modeling

Time profiles for the six variables of seven cell culture runs in 5,000-L bioreactors were used to establish the kinetic model (training data set) as presented in Figure 2. Overall, the cell growth curve was consistent with general mammalian cell growth patterns as it included exponential growth, stationary, and cell death phases (Figure 2A). The rate of B1 protein production was low until 170 h after which it increased exponentially (Figure 2B). Glucose and glutamine reached minimum concentrations at ~150 h. Afterward, glucose remained at a nearly constant level (Figure 2C), whereas glutamine accumulated (Figure 2D). Ammonia increased to a maximum concentration of ~5 mM and then leveled off (Figure 2E). However, lactate kept increasing through the end of cell culture period (Figure 2F).

Six kinetic constants (**P**) were calculated from the cell culture runs in 5,000-L bioreactors as shown in Table 2. A total of 112 cell culture runs were used to estimate μ_{max} and k_d.

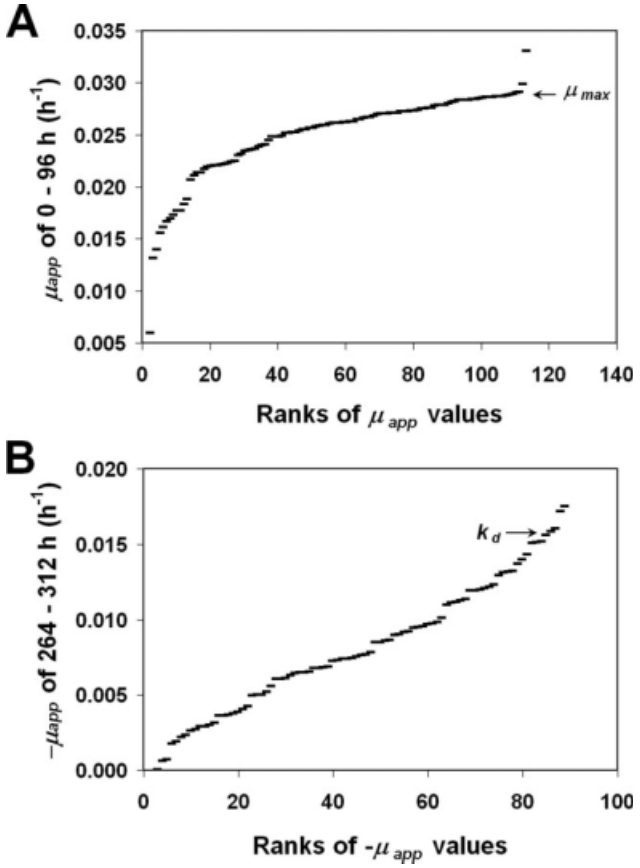

Figure 3. Demonstration of determining μ_{max} (A) and k_d (B) from 112 cell culture runs. Using the upper limit at the 95% confidence level, 106 out of 112 μ_{app} values (0–96 h) are less than μ_{max}, whereas 84 out of 89 $-\mu_{app}$ values (264–312 h) are less than k_d. Twenty-three runs were not used for k_d calculation due to earlier harvested.

As mentioned in the Materials and Methods section, the upper limit at the 95% confidence level for the μ_{app} between 0 and 96 h was defined as μ_{max}, whereas the upper limit at the 95% confidence level for the $-\mu_{app}$ between 264 and 312 h was defined as k_d. Figure 3A shows that 106 out of 112 μ_{app} values in 0–96 h were less than 0.029 h^{-1}, thus μ_{max} value was 0.029 h^{-1}. Figure 3B shows that 84 out of 89 $-\mu_{app}$ values between 264 and 312 h were less than 0.016 h^{-1}, thus k_d value was 0.016 h^{-1}. The other 23 cell culture runs were not used for k_d calculation due to earlier harvest. The values of $Y_{X_v/glc}$, $Y_{X_v/gln}$, $Y_{lac/glc}$, and $Y_{amm/gln}$ were calculated in the exponential growth phase ($d \leq 6$) for each cell culture run using Eq. 4. The average values of 14 cell culture runs are presented in Table 2.

The kinetic model (Eq. 6) was employed for each time period between two successive feedings ($t^{(d)}$, $t^{(d+1)}$) of the fed-batch culture. The inputs were values of the six variables at $t^{(d)}$ ($\mathbf{X1^{(d)}}$) and six constants (**P**). As shown in Figure 1B and Eq. 6, the single solution of simulated values of the six variables at $t^{(d+1)}$ ($\mathbf{X2^{(d+1)}}$) were obtained using a set of the 12 proposal parameters (θ). In addition, the evaluation of 12 proposal parameters was based on the agreement between the simulated and the measured values of 78 measurements (six variables at 13 sampling points) in MCMC sampling process as shown in Figure 1A. The number of measurements was greater than the number of parameter to be

Table 3. Model Parameters Estimated by MCMC Sampling Procedure

Parameter	Range* θ_i^{min}	Range* θ_i^{max}	Initial Value†	True Value	Values in Literature‡
For cell growth					
K_{glc} (mM)	0.001	0.15	0.25, 0.50, 0.75	0. 084 ± 0.004	0.15–1.00
K_{gln} (mM)	0.001	0.06	0.2, 0.4, 0.6	0.047 ± 0.004	0.06–0.80
KI_{amm} (mM)	3.0	10.0	4.8, 6.5, 8.3	6.51 ± 0.03	1.0–20.0
KI_{lac} (mM)	40.0	100.0	55, 70, 85	43.0 ± 2. 5	8.0–140.0
For cell death					
KD_{amm} (mM)	3.0	10.0	4.8, 6.5, 8.3	6.51 ± 0.02	1.44–4.50
KD_{lac} (mM)	40.0	100.0	55, 70, 85	45.8 ± 4.1	15.0–311.0
For cell maintenance					
m_{glc} (10^{-12} mmol cell^{-1} h^{-1})	0.5	100	25, 50, 75	69.2 ± 9.0	0–200
a_1 (10^{-12} mmol cell^{-1} h^{-1})	0.1	15	3.8, 7.6, 11.3	3.2 ± 1.1	0–340
a_2 (mM)	0.20	4.00	1.2, 2.1, 3.1	2.1 ± 0.2	0.2–4.0
For chemical degradation and mechanical removal					
d_{gln} (10^{-3} h^{-1})	1	10	3.3, 5.5, 7.8	7.2 ± 0.4	4.3–4.8
r_{amm} (10^{-12} mmol cell^{-1} h^{-1})	0.01	20	6, 10, 15	6.3 ± 1.0	N/A
For B1 production					
Q_{B1} (10^{-12} L cell^{-1} h^{-1})	0.001	0.04	0.01, 0.02, 0.03	4.0 ± 0.5	N/A

* The values of θ_i^{min} and θ_i^{max} are adopted from literature[1,2,38] or based on the cell culture data used in this study. † The initial values of a parameter are in order for the 1st, 2nd, and 3rd sampling trains, which are the cutoff values of 25, 50, and 75% of the parameter range. ‡ The parameters reported in literature for mammalian cell cultures.[11,21,40]

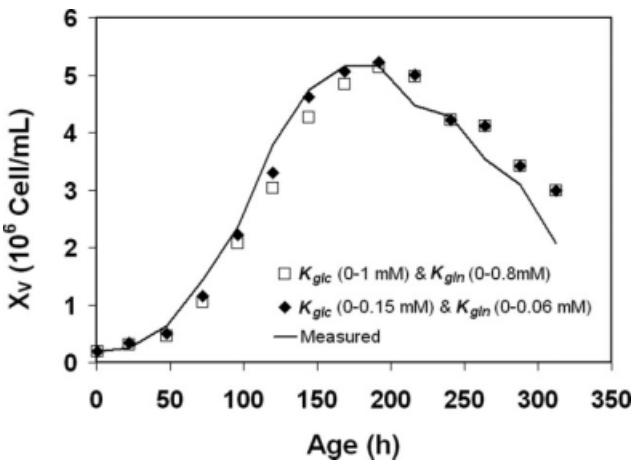

Figure 4. Effects of different upper bounds for K_{glc} and K_{gln} on viable cell density in the MCMC sampling procedure.

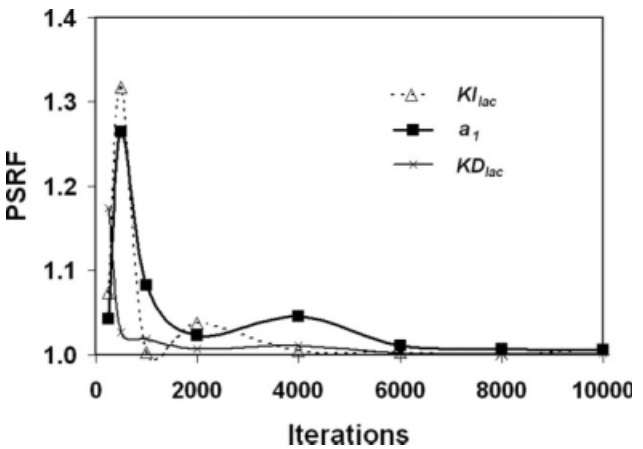

Figure 5. PSRF values for the cell culture run #4 with 10,000 iterations. Among 14 parameters, three parameters that required the most iteration numbers to reach a steady state (PSRF = 1) are presented.

evaluated, which ensured the single solution of the parameter estimation.

Reliability and applicability assessments of the kinetic model

MCMC sampling was key component in the current kinetic modeling work, which was performed for each cell culture run of the training data-set (seven runs). The assessments of the reliability of the kinetic model were examined from three perspectives. The first assessment was based on the selection of a parameter space (θ_i^{min} and θ_i^{max}) as the range of each parameter. The values for θ_i^{min} and θ_i^{max} for all 12 parameters, which were adopted mainly from literature values,[1,2,38] are presented in Table 3. The upper bound for the ammonia removal rate, r_{amm} (20×10^{-12} mmol cell^{-1} h^{-1}) was set to cover the maximum ammonia production rate based upon the peak specific glutamine consumption rate after 90 h (26×10^{-12} mmol cell^{-1} h^{-1}) and $Y_{amm/gln}$ (0.67). The upper bounds of K_{glc} (0.15 mM) and K_{gln} (0.06 mM) used in this work were the lowest values reported in literature.[11] Before the modeling, the higher values of upper bounds for K_{glc} (1 mM) and K_{gln} (0.8 mM) were examined, which are the highest values reported in literature.[11] Figure 4 shows that the viable cell density in the period 120–168 h was underestimated using the upper bound values of 1 mM for K_{glc} and 0.8 mM for K_{gln}. Using upper bound values of 0.15 mM for K_{glc} and 0.06 mM for K_{gln}, the fit for viable cell density was improved.

The second assessment was based on the iteration numbers needed for the MCMC sampling to reach a steady state. Three MCMC sampling trains were used for each cell culture run. As shown in Table 3, the initial values of 25, 50, and 75% of the parameter ranges were used for the first, second, and third sampling trains, respectively. With this approach, MCMC sampling reaches a steady state if PSRF values approach one, suggesting that the estimated 12 model parameters were equivalent among three independent sampling trains. Figure 5 illustrates the assessment using a cell culture run #4 as an example. Among the 12 estimated parameters, three parameters (KI_{lac}, a_1, and KD_{lac}) required the most iteration numbers for the PSRF values to approach one.

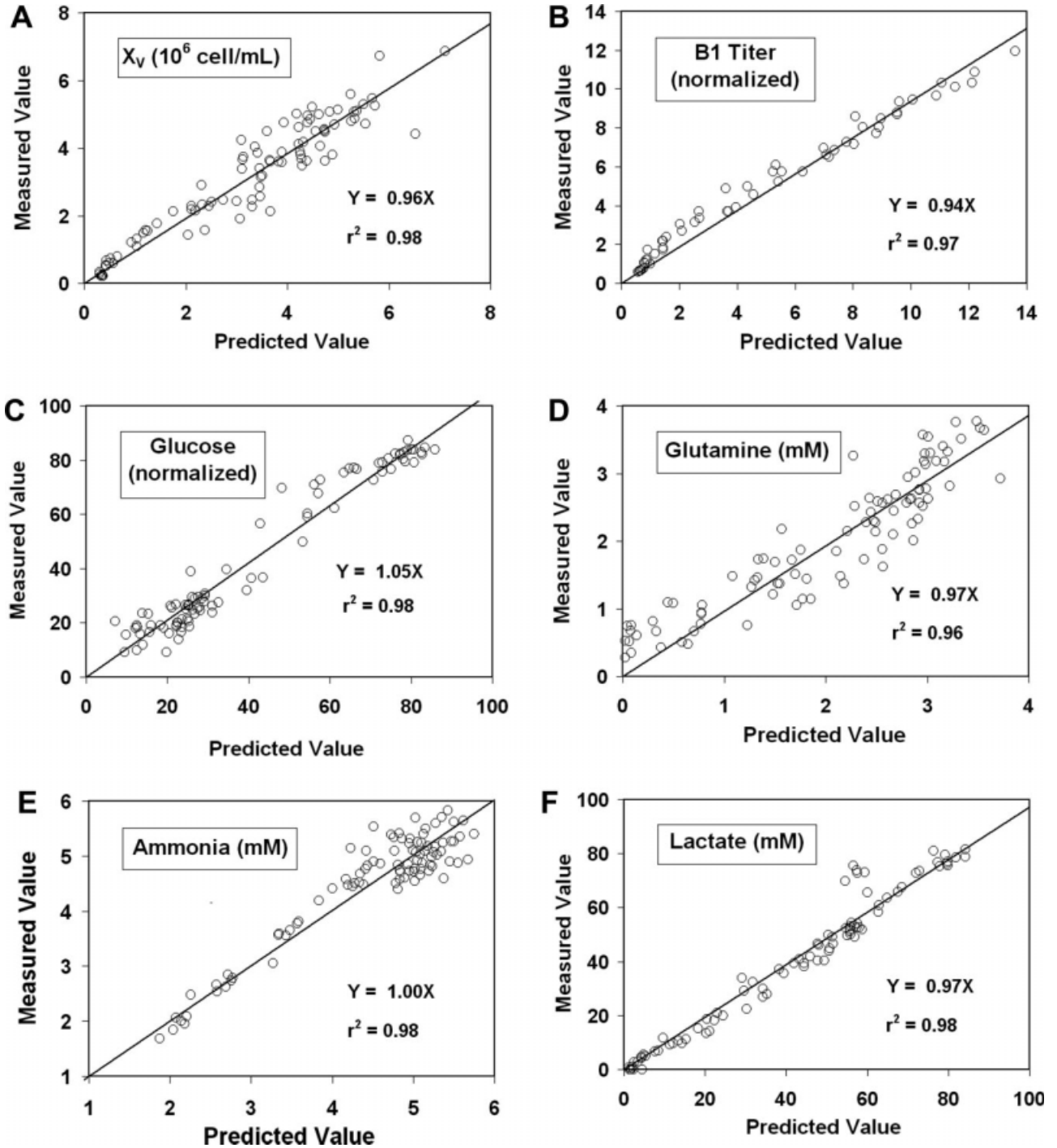

Figure 6. The simulated and measured values of six variables in the training data set. The simulated values were calculated by Eq. 6 using estimated parameters. Ninety-one points were plotted for each variable (7 runs each including 13 time points).

Apparently, MCMC sampling for this cell culture run reached a steady state after 6,000 iterations based on PSRF values. In this study, MCMC sampling with 10,000 iterations was used for all seven of the cell cultures in the training data-set. All 84 PSRF-values (12 parameters from seven cell culture runs) fell in the range of 1.00 and 1.06, indicating that the estimates were consistent after 10,000 iterations.

The third assessment was based on the accuracy of the kinetic model. The parameters estimated by the MCMC method were based on the fit of the simulated values using the estimated parameters to the measured values of the training data set as shown in Eq. 12. Figure 6 shows the plots of measured values against simulated values for the six variables from the training data set. Although 56 measurements were plotted (seven cell culture runs at eight sampling times) for [B1], 91 measurements were plotted (seven cell culture runs at 13 sampling times) for the other five parameters. Since the titer measurements started after 140 h, there were fewer numbers of measurements for [B1] than for the other variables. All coefficients of determination (r^2) were greater than 0.96 and the slopes of the regression lines for all six variables were close to one (between 0.94 and 1.05) using the least-squared-error regression approach. This suggests that the simulated values were in agreement with the

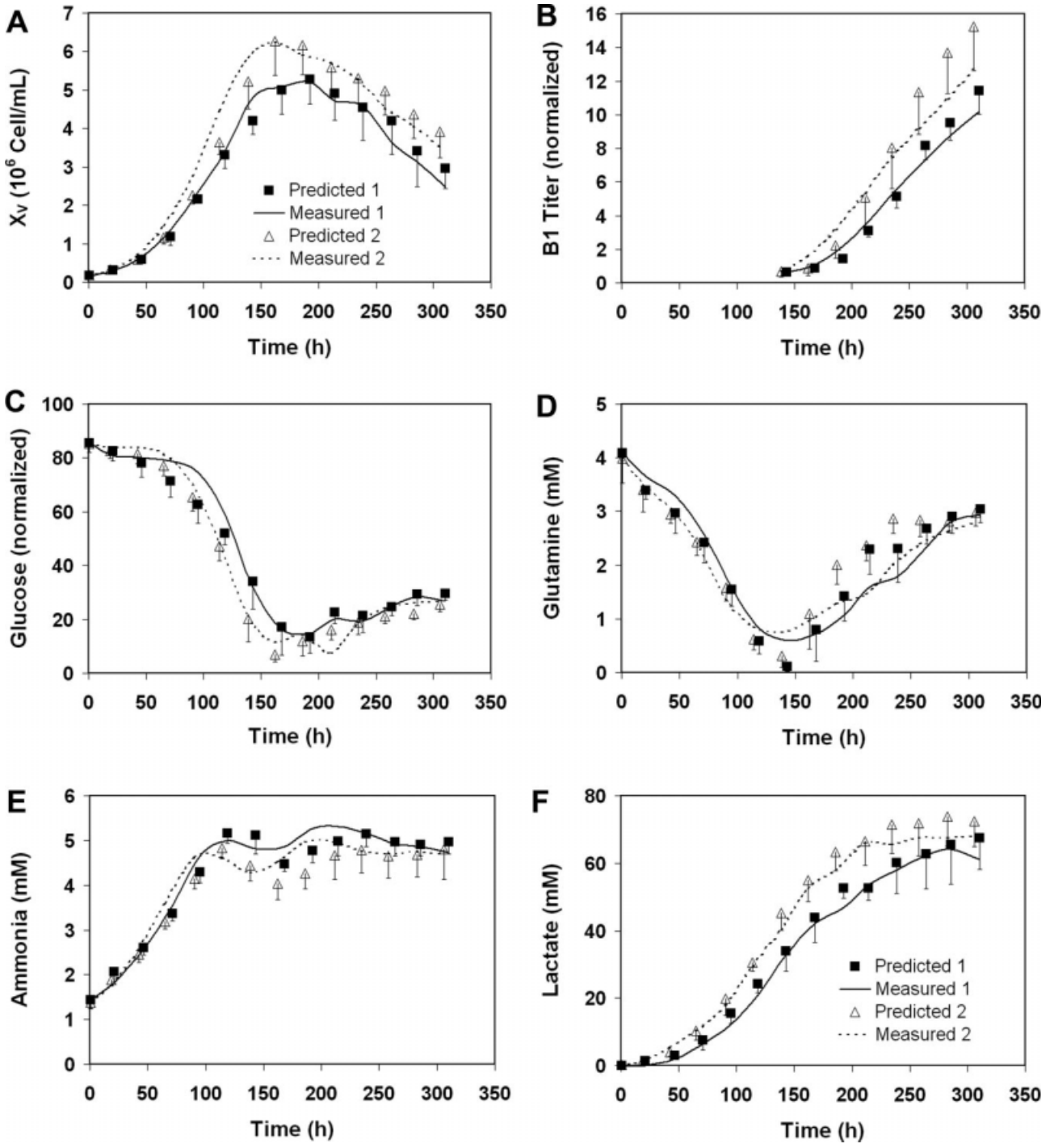

Figure 7. The measured and predicted time profiles of six variables in the validation date sets. Cell cultures of the first validation data set (Validation 1) were performed in 5,000 L bioreactors (Predict 1 and Measured 1), whereas those of the second validation data set (Validation 2) were performed in 500 L bioreactors (Predict 2 and Measured 2). Each data set comprised seven cell culture runs. The bars are the standard deviations of the predicted values.

measured values in the training data-set at the 95% confidence level.

Finally, the applicability of the kinetic model was evaluated using two validation data sets at 5,000 L (Validation 1) and 500 L scales (Validation 2), respectively. Each data set consisted of seven cell culture runs. As shown in Figure 2, the time profiles of the six variables of Validation 1 were similar to the training data set, whereas profiles of Training 2 were different, which reflected perturbations of the cell culture condition. Even though both 500- and 5,000-L bioreactors have the same bioreactor configuration, the scaled agitation rate, and the same volume per volume per minute of air flow rate, the different metabolites profiles and lower viable cell density and B1 protein titer were observed in 5,000-L bioreactors, which was caused by inadequate mixing in 5,000-L bioreactors as previously reported.[47] The predicted time profiles agreed with the measured time profiles for the six variables in both validation data sets as shown in Figure 7, confirming the applicability of the kinetic model to the cell cultures under different cell culture conditions. In addition, the times profiles of the six variables in 500-L scale were similar to that of the 50 L scale as previously

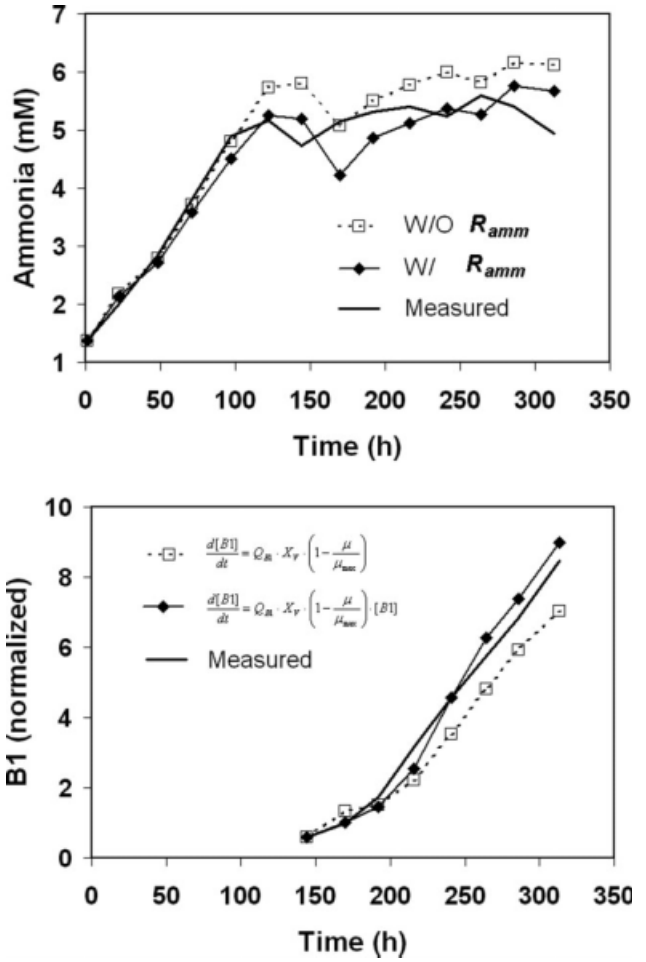

Figure 8. Comparison of the kinetic model with the alternative models with eliminating r_{amm} (A) and using the linear function of [B1] (open square in B). The cell culture run #4 was used as an example.

reported,[38] thus, the kinetic model may be generally applied at 50-L though 5,000-L scales.

Ammonia removal and [B1] protein production in the kinetic model

In addition to the MCMC methodology, the kinetic model uniquely incorporated a term for ammonia removal in the ammonia mass balance and an exponential function for [B1] (Eq. 6). An alternative model without the ammonia removal rate (r_{amm}) was evaluated and resulted in an overestimation for [AMM] values (Figure 8A). Ammonia is present as NH_4^+ (protonated ammonium) and NH_3 (unprotonated ammonia). Although approximately 1% of the total concentration of ammonia and ammonium is present as NH_3 (unprotonated ammonia) at the physiological pH of 7.1–7.5, the protonation and deprotonation reactions are extremely fast.[48] Therefore, the removal of NH_3 by gas sparging would drive the deprotonation reaction to continuously convert NH_4^+ to NH_3. Assuming a constant specific oxygen uptake rate, oxygen demand increases with viable cell density, which requires an increase in the bottom oxygen sparging rates. Therefore, ammonia removal can be dependent on the viable cell density. On the basis of the average specific glutamine consumption rate (10×10^{-12} mmol cell^{-1} h^{-1}) after 190 h and $Y_{amm/gln}$ (0.67), the value of r_{amm} (6.3×10^{-12} mmol cell^{-1} h^{-1}) indicates that ammonia removal can play an important role in the mass balance of ammonia.

The [B1] protein mass balance was expressed as an exponential function of [B1] in Eq. 6. Tatiraju et al.[40] defined the mass balance for a monoclonal antibody (MAb) as a linear function of [MAb]. Simon and Karim[9] also defined the t-PA protein mass balance as a linear function of [t-PA] but with the slope of $\alpha(dX_V/dt) + \beta X_V$, where α and β are growth-associated and nongrowth-associated constants, respectively. However, Jang and Barford[21] reported the MAb mass balance using an exponential function of [MAb]. For current study, both linear and exponential functions were evaluated as shown in Figure 8B. The result indicated that the linear function for [B1] protein mass balance underestimated [B1] values, whereas the exponential function (Eq. 6) resulted in an improved fit with the measured data.

In addition, the term $(1-\mu/\mu_{max})$ was used to represent the fraction of arrested viable cells for the [B1] protein mass balance in Eq. 6. It has been reported that the specific antibody production rate was highest in the G1-phase[20] or G0-phase of cell cycle.[21] Comprehensive details of the cell cycle in mammalian cells have been described elsewhere.[49] Briefly, if appropriate growth factors are not available in G1, the cell cycle stops at the restriction point. Such arrested cells then enter the quiescent G0 stage for a long period of time without proliferating.[49] Assuming all viable cells are dividing in exponential growth phase with the specific growth rate of μ_{max}, the term of $(1-\mu(t)/\mu_{max})X_v$ represents the proportion of arrested viable cells at time t. Without the term $(1-\mu(t)/\mu_{max})$, the simulated values did not fit the measured values of [B1] (data not shown). The expression of [B1] in the mass balance of Eq. 6 suggests that the arrested viable cell numbers positively correlated to the production rate for [B1]. Thus, a sustained high viable cell density may be critical to enhance B1 productivity.

Application of kinetic model in medium and process improvement

Ammonia and lactate were previously reported as the major inhibitory metabolites in this CHO cell culture process.[37,38] The kinetic model presented here was consistent with the observations in other cell culture systems, that the Monod equations are generally applicable for the modeling kinetics of cell cultures.[8,9,11] The kinetic model also elucidated that ammonia and lactate are the major factors in the Monod equations and hence play critical roles in cell growth and cell death.

Since the lactate and ammonia production positively correlated with the glucose and glutamine consumption rates, the use of minimum glucose and glutamine concentrations was recommended in several mammalian cell culture systems.[7,50] The estimated values of K_{glc} (0.084 mM) and K_{gln} (0.047 mM) for cell growth were much lower than the apparent K values of glutaminase for glutamine (2.0–4.5 mM) and the glycolytic pathways for glucose (2.0 mM), respectively. To reduce ammonia and lactate production in mammalian cell culture, Xie and Wang[50] suggested that twice the values for K_{glc} and K_{gln} be used as the initial concentrations for glutamine and glucose in the medium. Therefore, the estimated K_{glc} and K_{gln} values in this study suggests concentrations of [GLC] and [GLN] of 0.17 and 0.09 mM be used to reduce lactate and ammonia production in the current CHO cell culture process.

Glucose and glutamine consumption for cell maintenance was another factor addressed in this study. The glutamine maintenance coefficient (m_{gln}) is not a constant. Instead, it is a function of glutamine with constants a_1 (3.2×10^{-12} mmol cell^{-1} h^{-1}) and a_2 (2.1 mM) as shown in Eq. 8. The estimated average values of m_{gln} were within the range between 1.1 and 1.9×10^{-12} mmol cell^{-1} h^{-1} after 200 h based on a_1 and a_2. The measured glutamine consumption rate was 10×10^{-12} mmol cell^{-1} h^{-1} for the same period, which was much higher than the m_{gln} value. Therefore, the glutamine consumption for cell maintenance could be negligible. In contrast, the estimated value of m_{glc} was 69×10^{-12} mmol cell^{-1} h^{-1}. In comparison with the average of the glucose consumption rate after 200 h measured in this study (83×10^{-12} mmol cell^{-1} h^{-1}), approximately 83% of consumed glucose was used for cell maintenance in the late stage of cell culture. The high m_{glc} value suggests that the cells may be under stress after 200 h, which may be another area for process improvement.

Conclusion

A kinetic model using the MCMC method was developed for a large-scale CHO fed-batch culture process for the B1 fusion protein production. The fit of the predicted to the measured time profiles of six variables indicates that the kinetic model can be applied to the current fed-batch CHO cell culture process. This model uniquely incorporated a term for ammonia removal in the ammonia mass balance and an exponential function for B1 protein concentration. The estimated values for KI_{amm}, KD_{amm}, KI_{lac}, and KD_{lac} indicated that ammonia and lactate played critical roles on cell growth and cell death. The estimated values for K_{glc} and K_{gln} could also provide a basis for the initial medium design. The model indicated that 83% glucose uptake was used for cell maintenance during the late phase of the cell culture, whereas the glutamine maintenance coefficient was negligible. The kinetic model also suggests that it is critical for B1 production to sustain a high number of viable cells. Furthermore, the kinetic model was applicable in both validation data sets at 5,000-L and 500-L scales even though the time profiles of the six variables differed. Since the cell culture runs at the 500-L and 50-L had similar time profiles,[38] the kinetic model may be applied to cell cultures in 50-L bioreactors. From our knowledge, there are no literature reports on the kinetic parameters from CHO cell culture probably due to the difficulty of continuous cultures for multiple steady states even in laboratory bioreactors. It may be worthwhile to apply the MCMC methodology for the development of kinetic models in laboratory bioreactors of less than 50-L working volume.

Acknowledgments

The authors thank Drs. Michael Borys, Nicholas Abu-Absi, and Sarwat Khattak for helpful discussions on the manuscript.

Nomenclature

a_1 = constant parameter for Eq. 8, 10^{-9} mmol cell^{-1} h^{-1}
a_2 = constant parameter for Eq. 8, mM
CF_i = concentration of the ith variable in the feeding medium
Q_{B1} = specific B1 production rate (10^{-9} L cell^{-1} h^{-1})
k_d = maximum cell death rate, h^{-1}
KD_{amm} = half-maximum-rate concentration of ammonia for cell death rate, mM
KD_{lac} = half-maximum-rate concentration of lactate for cell death rate, mM
d_{gln} = first-order decomposition rate of glutamine, h^{-1}
K_{glc} = half-maximum-rate concentration of glucose for cell growth rate, mM
K_{gln} = half-maximum-rate concentration of glutamine for cell growth rate, mM
KI_{amm} = half-maximum-rate concentration of ammonia for cell growth rate, mM
KI_{lac} = half-maximum-rate concentration of lactate for cell growth rate, mM
m_{glc} = glucose maintenance coefficient, 10^{-9} mmol cell^{-1} h^{-1}
m_{gln} = glutamine maintenance coefficient, 10^{-9} mmol cell^{-1} h^{-1}
$\mathbf{P}$ = vector of calculated six constants for parameter estimation
PRSF = potential scale reduction factor
r_{amm} = ammonia removal rate, 10^{-9} mmol cell^{-1} h^{-1}
$t^{(d)}$ = sampling time on the dth day, h
$\mathbf{X1}^{(d)}$ = vector of calculated postfeeding values of 6 variables after daily feeding on the dth day
$x1_i^{(d)}$ = the ith variable value in $\mathbf{X1}^{(d)}$
$\mathbf{X2}^{(d)}$ = vector of measured pro-feeding values of 6 variables before daily feeding on the dth day
$x2_i^{(d)}$ = the ith variable value in $\mathbf{X2}^{(d)}$
$\hat{\mathbf{X}}2^{(d)}$ = vector of simulated pro-feeding values of 6 variables before daily feeding on the dth day
$\hat{x}2_i^{(d)}$ = the ith variable values in $\hat{\mathbf{X}}2^{(d)}$
V = culture volume in bioreactor, L
V_f = feeding volume, L
X_V = viable cell density, 10^9 cells L^{-1}
$Y_{amm/gln}$ = ammonia yield from glutamine, mol/mol
$Y_{lac/glc}$ = lactate yield from glucose, mol/mol
$Y_{Xv/glc}$ = glucose yield coefficient, cell L^{-1} mM^{-1}
$Y_{Xv/gln}$ = glutamine yield coefficient, cell L^{-1} mM^{-1}

Greek Letters

θ = vector of 12 model parameters
θ_i = the ith parameter value in θ
$\hat{\boldsymbol{\theta}}$ = vector of 12 proposal parameters
$\hat{\theta}_i$ = the ith parameter value in $\hat{\boldsymbol{\theta}}$
$\sigma_{\hat{\theta}}$ = vector of standard deviations of 12 proposal parameters
σ_i = standard deviation of the ith variable
τ = coefficient of variation
μ = specific cell growth rate (h^{-1})
μ_{app} = apparent cell growth rate (h^{-1})
μ_d = specific cell death rate (h^{-1})
μ_{max} = maximum specific cell growth rate (h^{-1})

Literature Cited

1. Miller WM, Blanch HW, Wilke CR. A kinetic analysis of hybridoma growth and metabolism in batch and continuous suspension culture: effect of nutrient concentration, dilution rate, and pH. *Biotechnol Bioeng*. 1988;32:947–965.
2. Bree MA, Dhurjati P, Geoghegan RF, Robnett B. Kinetic modelling of hybridoma cell growth and immunoglobulin production in a large-scale suspension culture. *Biotechnol Bioeng*. 1988;32: 1067–1072.
3. Batt BC, Kompala DS. A structured kinetic modeling framework for the dynamics of hybridoma growth and monoclonal antibody production in continuous suspension culture. *Biotechnol Bioeng*. 1989;34:515–531.
4. Glacken MW, Huang C, Sinskey AJ. Mathematical descriptions of hybridoma culture kinetics. III. Simulation of fed-batch bioreactor. *J Biotechnol*. 1989;10:39–66.
5. Frame KK, Hu WS. Kinetic study of hybridoma cell growth in continuous culture. I. A model for nonproducing cells. *Biotechnol Bioeng*. 1991;37:55–64.

6. Sanderson CS, Barton GW, Barford JP. Optimization of animal cell culture media using dynamic simulation. *Comput Chem Eng*. 1995;19:s681–s686.
7. Zeng AP, Deckwer WD. Mathematical modeling and analysis of glucose and glutamine utilization and regulation in cultures of continuous mammalian cells. *Biotechnol Bioeng*. 1995;47: 334–346.
8. Marique T, Cherlet M, Hendrick V, Godia F, Kretzmer G, Werenne J. A general artificial neural network for the modelization of culture kinetics of different CHO strains. *Cytotechnology*. 2001;36:55–60.
9. Simon L, Karim MN. Control of starvation-induced apoptosis in Chinese Hamster Ovary cultures. *Biotechnol Bioeng*. 2002;78: 645–657.
10. Sidoli FR, Mantalaris A, Asprey SP. Modelling of mammalian cells and cell culture processes. *Cytotechnology*. 2004;44:27–46.
11. Pörtner R, Schäfer T. Modelling hybridoma cell growth and metabolism - a comparison of selected models and data. *J Biotechnol*. 1996;49:119–135.
12. Barford JP, Hall RJ. An evaluation of the approaches to the mathematical modelling of microbial growth. *Process Biochem*. 1978;18:22–29.
13. Ray NG, Karkare SB, Runstadler PW. Cultivation of hybridoma cells in continuous cultures: kinetics of growth and product formation. *Biotechnol Bioeng*. 1989;33:724–730.
14. Bibila T, Flickinger MC. A structured model for monoclonal antibody synthesis in exponentially growing and stationary phase hybridoma cells. *Biotechnol Bioeng*. 1991;37:210–226.
15. Hayter PM, Kirkby NF, Spier RE. Relationship between hybridoma growth and monoclonal antibody production. *Enzyme Microb Technol*. 1992;14:454–461.
16. Garatun-Tjeldstø O, Pryme IF, Weltman JK, Dowben RM. Synthesis and secretion of light-chain immunoglobulin in two successive cycles of synchronized plasmacytoma cells. *J Cell Biol*. 1976;68:232–239.
17. Golding B, Pillemer SR, Roussou P, Peters EA, Tsokos GC, Ballow JE, Hoffman T. Inverse relationship between proliferation and differentiation in a human TNP-specific B cell line. Cell cycle dependence of antibody secretion. *J Immunol*. 1988; 141:2564–2568.
18. Ramírez OT, Mutharasan R. Cell cycle- and growth phase-dependent variations in size distribution, antibody productivity, and oxygen demand in hybridoma cultures. *Biotechnol Bioeng*. 1990;36:839–848.
19. Linardos TI, Kalogerakis N, Behie LA. Cell cycle model for growth rate and death rate in continuous suspension hybridoma cultures. *Biotechnol Bioeng*. 1992;40:359–368.
20. Suzuki E, Ollis DF. Cell cycle model for antibody production kinetics. *Biotechnol Bioeng*. 1989;34:1398–1402.
21. Jang JD, Barford JP. An unstructured kinetic model of macromolecular metabolism in batch and fed-batch cultures of hybridoma cells producing monoclonal antibody. *Biochem Eng J*. 2000;4:153–168.
22. Dalili M, Sayles GD, Ollis DF. Glutamine-limited batch hybridoma growth and antibody production: experiment and model. *Biotechnol Bioeng*. 1990;36:74–82.
23. Frame KK, Hu WS. Kinetic study of hybridoma cell growth in continuous culture. II. Behavior of producers and comparison to nonproducers. *Biotechnol Bioeng*. 1991;38:1020–1028.
24. Hiller GW, Aeschlimann AD, Clark DS, Blanch HW. A kinetic analysis of hybridoma growth and metabolism in continuous suspension culture on serum-free medium. *Biotechnol Bioeng*. 1991;38:733–741.
25. Kurokawa H, Park YS, Lijima S, Kobayashi T. Growth characteristics in fed-batch culture of hybridoma cells with control of glucose and glutamine concentration. *Biotechnol Bioeng*. 1994; 44:95–103.
26. Ludemann I, Portner R, Markl H. Effect of NH_3 on the cell growth of a hybridoma cell line. *Cytotechnology*. 1994;14:11–30.
27. Omasa T, Higashiyama KI, Shioya S, Suga KI. Effects of lactate concentration on hybridoma culture in lactate-controlled fed-batch operation. *Biotechnol Bioeng*. 1992;39:556–564.
28. Heidemann R, Lütkemeyer D, Büntemeyer H, Lehmann J. Effects of dissolved oxygen levels and the role of extra- and intracellular amino acid concentrations upon the metabolism of mammalian cell lines during batch and continuous cultures. *Cytotechnology*. 1998;26:185–197.
29. Provost A, Bastin G, Agathos SN. Metabolic design of macroscopic bioreaction models: application to Chinese hamster ovary cells. *Bioprocess Biosyst Eng*. 2006;29:349–366.
30. Goudar CT, Joeris K, Konstantinov KB, Piret JM. Logistic equations effectively model mammalian cell batch and fed-batch kinetics by logically constraining the fit. *Biotechnol Prog*. 2005; 21:1109–1118.
31. Holmberg A. On the practical identifiability of microbial growth models incorporating Michaelis-Menten type nonlinearities. *Math Biosci*. 1982;62:23–43.
32. Liu C, Zachara JM. Uncertainties of Monod kinetic parameters nonlinearly estimated from batch experiments. *Environ Sci Technol*. 2001;35:133–141.
33. Cappuyns AM, Bernaerts K, Smets IY, Ositadinma O, Prinsen E, Vanderleyden J, Van Impe JF. Optimal fed batch experiment design for estimation of Monod kinetics of *Azospirillum brasilense*: from theory to practice. *Biotechnol Prog*. 2007;23:1074–1081.
34. Skolpap W, Scharer JM, Douglas PL, Moo-Young M. Fed-batch optimization of α–amylase and protease-producing *Bacillus subtilis* using Markov chain methods. *Biotechnol Bioeng*. 2004;86: 706–717.
35. Coleman MC, Block DE. Bayesian parameter estimation with informative priors for nonlinear systems. *AIChE J*. 2006;52: 651–667.
36. Anderson KE, Højbjerre H. A population-based Bayesian approach to the minimal model of glucose and insulin homeostasis. *Stat Med*. 2005;24:2381–2400.
37. Zhu MM, Goyal A, Rank DL, Gupta SK, Vanden Boom T, Lee SS. Effects of elevated pCO_2 and osmolality on growth of CHO cells and production of antibody-fusion protein B1: a case study. *Biotechnol Prog*. 2005;21:70–77.
38. Xing Z, Li Z, Chow V, Lee SS. Identifying inhibitory threshold values of repressing metabolites in CHO cell culture using multivariate analysis methods. *Biotechnol Prog*. 2008;31:675–683.
39. Sauer PW, Burky JE, Wesson MC, Sternard HD, Qu L. A high-yielding, generic fed-batch cell culture process for production of recombinant antibodies. *Biotechnol Bioeng*. 2000;67:585–597.
40. Tatiraju S, Soroush M, Mutharasan R. Multi-rate nonlinear state and parameter estimation in a bioreactor. *Biotechnol Bioeng*. 1999;63:22–32.
41. Shuler ML, Kargi F. *Bioprocess Engineering: Basic Concepts*, 2nd ed. Upper Saddle River, NJ: Prentice Hall; 2002.
42. Ridgeway G, Madigan D. A sequential Monte Carlo method for Bayesian analysis of massive datasets. *J Data Min Knowl Discov*. 2003;7:301–319.
43. Bois FY, Smith TJ, Gelman A, Chang HY, Smith AE. Optimal design for a study of butadiene toxicokinetics in humans. *Toxicol Sci*. 1999;49:213–224.
44. Brooks SP, Gelman A. General methods for monitoring convergence of iterative simulations. *J Comput Graph Stat*. 1998;7: 434–455.
45. Brooks SP, Roberts GO. Convergence assessment techniques for Markov chain Monte Carlo. *Stat Comput*. 1998;8:319–335.
46. Linko S, Luopa J, Zhu YH. Neural networks as 'software sensors' in enzyme production. *J Biotechnol*. 1997;52:257–266.
47. Xing Z, Kenty BK, Li ZJ, Lee SS. Scale-Up analysis for a CHO cell culture process in large-scale bioreactors. *Biotechnol Bioeng*. 2009;103:733–746.
48. Schneider M, Marison IW, von Stockar U. The importance of ammonia in mammalian cell culture. *J Biotechnol*. 1996;6:161–185.
49. Cooper GM. *The Cell: A Molecular Approach*. Washington, DC: ASM Press; 1997.
50. Xie L, Wang DIC. Fed-batch cultivation of animal cells using different medium design concepts and feeding strategies. *Biotechnol Bioeng*. 1994;43:1175–1189.

Manuscript received Nov. 26, 2008, and revision received Apr. 8, 2009.